32nd Electric Vehicle Symposium (EVS32)
Lyon, France, May 19 - 22, 2019

Use of the advanced X-ray sources to accelerate the development of batteries and fuel cells for mobile applications.

Jakub Drnec*[1], Marco di Michiel[1] and Alexander Rack[1]
[1]*European Synchrotron Radiation Facility, 71 Avenue des Martyrs, 38000 Grenoble*
∗*Corresponding author*

Abstract

Batteries and fuel cells are one of the most important parts in electric vehicles due to their ability to provide the propelling power. Complete characterisation of these electrochemical devices in operando conditions is therefore necessary to guide the device development and to improve the driving range and charging speed of electric vehicles. Here we show several examples of how modern, high brilliance X-ray sources can be used to collect 3D snapshots of running electrochemical devices. This helps to understand their internal functioning and the processes leading to the device degradation. Structural and chemical tomographic information of bulk materials and interfaces is obtained at all length scales, ranging from centimeters to ngstroms, with sufficient temporal resolution. Experiments in operando conditions are used to understand the internal functioning of the device and to tune the operation conditions. Our tools developed at ESRF and tailored to probe electrochemical devices are available for all users from industry and academia.

Keywords: batteries, fuel cells, X-ray characterisation, synchrotron

1 Introduction

Our clean energy future greatly depends on the engineering and scientific progress in developing energy storage and conversion devices. Such devices, e.g. batteries and fuel cells, will form the integral part of our future energy grid. Given their flexibility, these are already being used in mobile and stationary applications. However due to the remaining shortcomings, the battery and fuel cell technology still lags behind the established fossil fuel solutions. In order to speed up the energy grid transition to renewable sources, these shortcomings needs to be eliminated.

In the case of batteries, specific energy, capacity and charging times need to be improved so this type of energy storage can be widely used in most vehicles, including the heavy duty transportation. For the fuel cells, the main obstacle is the price of the stack caused partially by the high loading of Platinum catalysts and the mediocre longevity. In both cases, these obstacles can be solved by advances in basic and applied research as well as engineering.

Structural and chemical analysis of the constituent materials is essential as this information guides the progress in material engineering. Furthermore, the ability to study the materials during the device functioning is indispensable as the materials often behave differently then in idealized laboratory conditions. Unfortunately, to obtain such information in complex environments still remains a challenge. The high

energy X-ray source at European synchrotron radiation facility can provide needed information for wide variety of energy related materials in idealized and operating conditions. Range of X-ray analytical techniques are available to gain information at various scales (angstroms to millimeters) and with high time resolution (up to ns). Multiple instruments are available for users from academia and industry, and testing devices dedicated to X-ray experiments are ready for immediate use [1]. In the following, we will provide various examples of experiments performed at ESRF in last years to give an overview of available techniques and approaches tailored to battery and fuel cell research.

2 Batteries

Battery failures are one of the most serious incidents which can threaten not only lives of the users, but also the proliferation of the battery technology in the mobility applications. Various experiments were performed at ESRF which helped to understand failure mechanisms, highlighting the general importance of safety design.

In the first example we will discuss the X-ray tomography experiment where the thermal runaway was monitored. The high photon flux allows image acquisition during very short period of time providing unprecedented temporal resolution. For the first time, the nucleation and propagation of failure was monitored in real time.

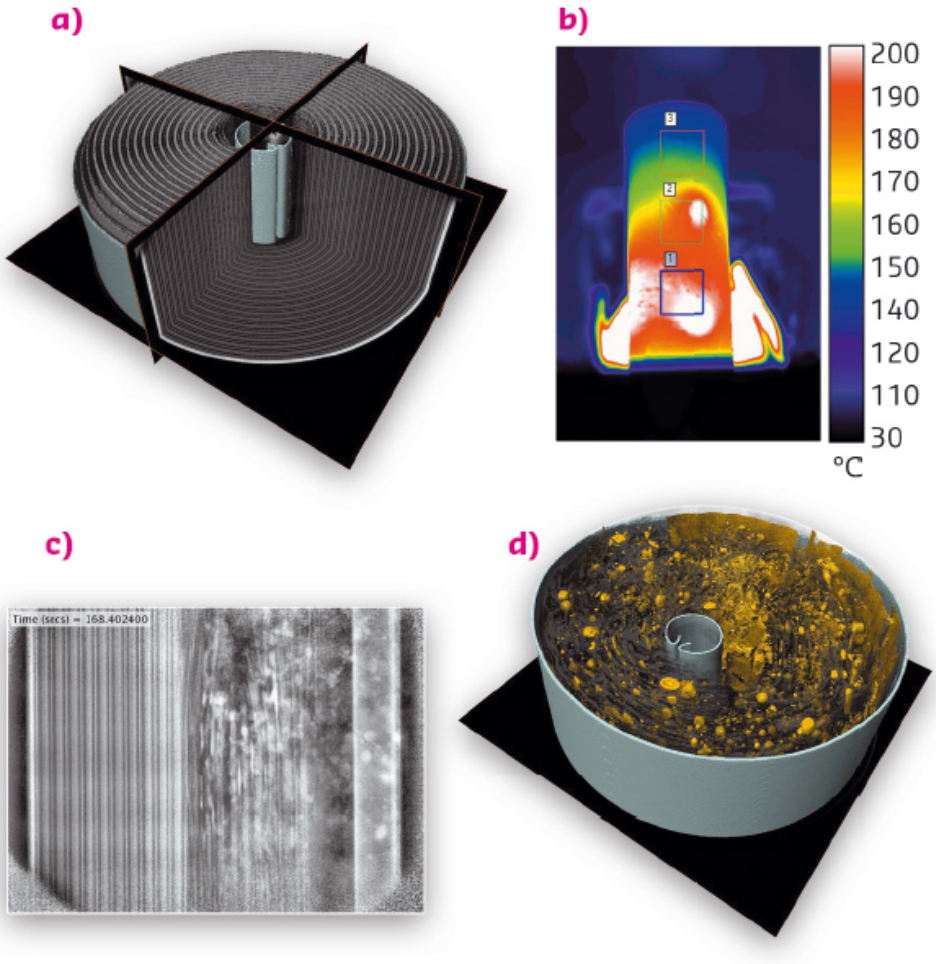

Figure 1: (a) 3D reconstruction of a fresh cell with internal cylindrical support, (b) thermal image of a failing cell, (c) radiograph showing the propagation of thermal runaway and (d) post-mortem 3D reconstruction.

It was found that an internal cylindrical support played an important role in improving the safety of a cell by providing structural support for the tightly wound electrode layer, and acting as a channel for gases to flow uninterrupted from the base of the cell to the vent during failure (Figure 1). Without the cylindrical

support the internal architecture collapsed after venting, the consequences of which include increased risk of thermal runaway due to exposure of cell material to air. [2]

The ability to control the location of runaway initiation also allowed examination of whether cells are at greater risk of undergoing side-wall rupture when thermal runaway initiates closer to the surface of the cell casing. X-ray images showed that when thermal runaway is initiated three layers deep into the cell, as opposed to six layers deep, its reaction front reaches the casing of the cell in less than 1/10th of the time. This has implications for early temperature-induced weakening of the steel casing and the formation of more favourable conditions for side-wall rupture to occur.[3]

Beside the ultra-fast computed tomography in operando conditions, we also routinely use advanced diffraction tomography techniques (XRD-CT) and experiments tailored to get the chemical information about the processes happening in the battery during the charge and discharge. These experiments are typically tailored to reveal the change of the chemical phase and volume of anode and cathode materials as well as changes happening at the interface between the materials consisting the battery [4, 5]. The example of XRD-CT reconstruction of Ni-MH battery cell is in Figure 2. All the battery materials are clearly distinguished (cathode (b), anode (c), steel (d), amorphous components (e)) and can be followed during the charge/discharge cycle.

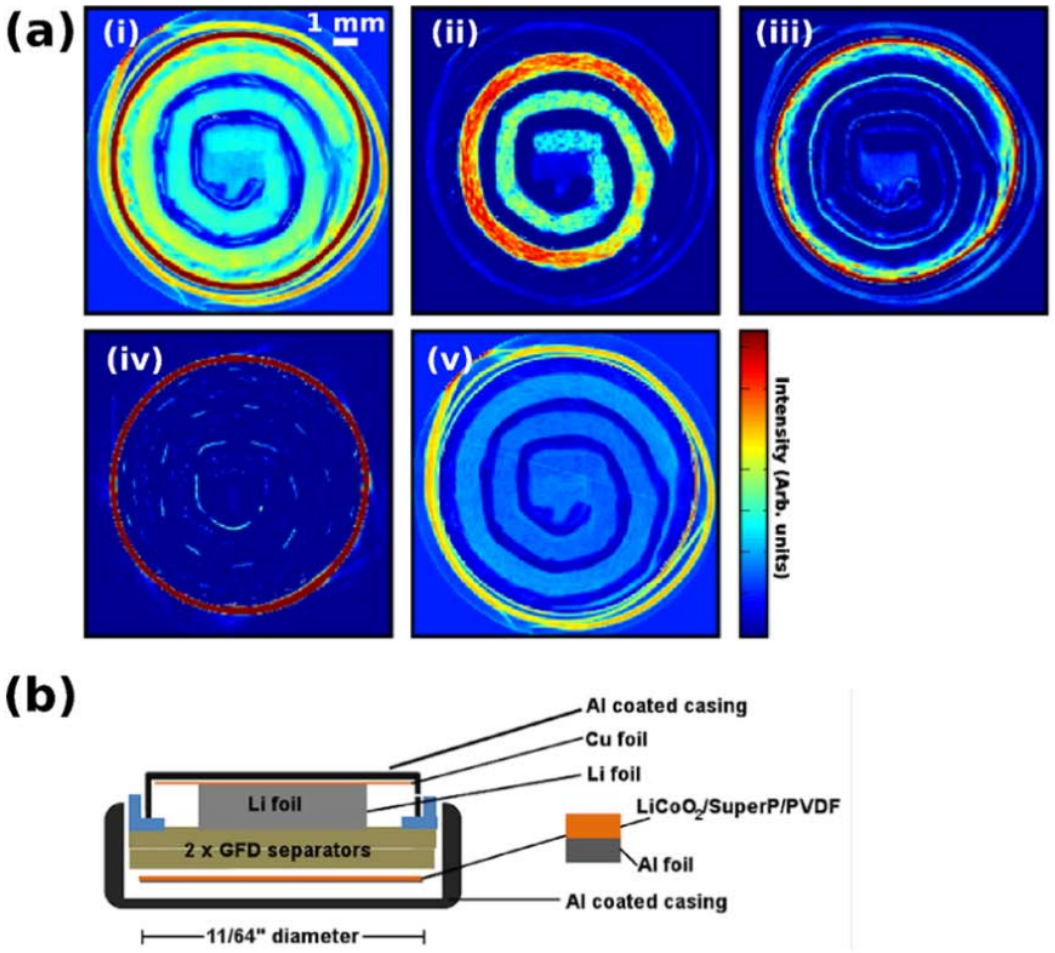

Figure 2: Data collected for cycled Ni-MH cell: (i) summed intensity in the q-range 20 to 23 1; (ii) intensity at q=1.36 1, representing the cathode phase;(iii) intensity at q=1.64 1, representing the anode phase; (iv) intensity at q=3.09 1, representing steel; (v) intensity at q=1.40 1, representing any amorphous component. (b) Schematic of coin cell assembly. Reproduced from [4]

3 Hydrogen Fuel Cells

The fuel cell ($5\,\mathrm{cm}^2$) running at $1.5\,\mathrm{A/cm}^2$ (automotive current densities) is investigated with high energy X-ray probe to image the conditions within the cell and to understand the processes leading to the degradation of the cathode catalyst. The high energy X-ray beam penetrates the whole fuel cell, which allows to use the advanced data acquisition and analysis techniques. By proper deconvolution of the diffraction patterns, we are able to recover the snapshots of the active materials and the water distribution within the cell. This helps to determine the chemical and mechanical connection between the different materials used in the MEA composite.

In the example (Figure 3) we show the water distribution within the channel and landed area at different operating conditions. The patterns were measured by vertically moving the sample through the beam. The sample flowfield (straight channels) was positioned parallel to the beam which means that one XRD pattern correspond to the beampath of $2.2\,\mathrm{cm}$ along the channel. These pattern were then deconvoluted by fitting the standards for each element of the cell (GDL,catalyst, catalyst support, Nafion and water), together with the compton background and diffuse air scattering, to each XRD pattern.

Plot (a) shows the water distribution under the channel while the cathode's relative humidity is changed. Note that the flowfields of anode and cathode are aligned in a such way that the cathode channels are directly above the anode channels. The deconvoluted signal from the carbonous materials in the MEA (pink curve) traces the profile of the flowfield (graphite) and the GDL (Sigracet, $20\,\mu\mathrm{m}$ thickness). The Nafion in the middle of the cell is in between $6.05\,\mathrm{mm}$ and $6.2\,\mathrm{mm}$, where the carbon signal is 0. The relative humidity (RH) on the anode side is kept at 100% and the flow of both H_2 (anode) and O_2 (cathode) is $600\,\mathrm{sccm}$. The cell is running at current density of $2\,\mathrm{A/cm}^2$. At RH 90% on the cathode side (light blue curve) the water unexpectedly condensate in the GDL of the anode side rather then increasing the water content on the cathode side. We assign this effect to the sufficient diffusion of the water, generated on the cathode at high current densities, to the anode side. As the RH on the anode is already at RH 100%, this further addition of water from the cathode causes flooding of the anode GDL. The water diffusion through the Nafion membrane is likely accelerated due the the very small thickness in the shown case and membranes with different thicknesses will behave differently.

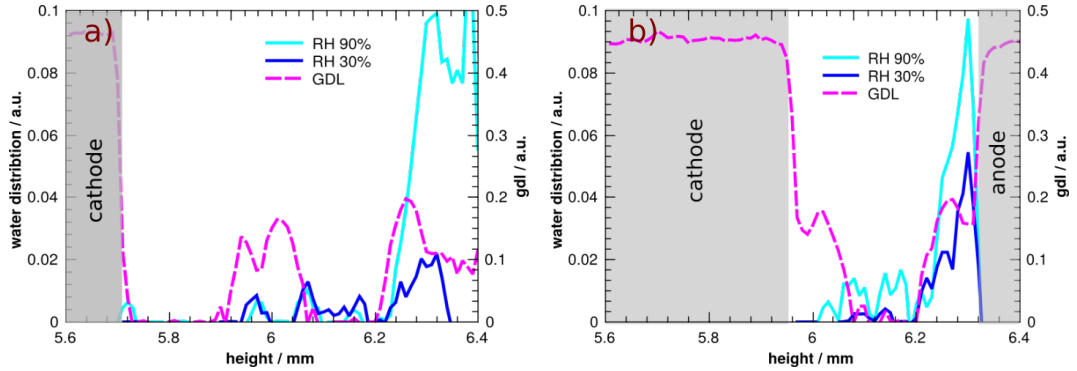

Figure 3: Water distribution in the channel (a) at two operating conditions: 90% relative humidity on the cathode and 30% relative humidity on the anode. The relative humidity (RH) on the anode side is kept at 100% and the flow of both H_2 (anode) and O_2 (cathode) is $600\,\mathrm{sccm}$. The cell is running at current density of $2\,\mathrm{A/cm}^2$. The plot (b) shows the same for the landed area. Signal from carbon materials (GDL) is also shown in the plot for better orientation.

When the RH on the cathode side is changed to 30%, the water generated on the cathode will diffuse faster to the cathode GDL due to the lower RH in the cathode channel. Most of the generated water is then displaced to the this side, and the diffusion to the anode side diminish, causing the water content in the anode GDL to drop (dark blue curve).

The water content under the landed during the RH change is shown in plot (b). Here we observe similar behaviour than in the channel, but the at RH 30% the water is not completely removed from under the landed area and the landed areas of the cell generally contain more water. This follows the previous observations done by neutron imaging where the authors show that the landed areas trap water.

By using advanced tomography techniques, the 3D reconstruction based on the diffraction patterns is also possible. In this approach a small pencil-like beam is rastered through the cell at different azimuthal angles. The typical back-projection algorithm is used to reconstruct the 2D slices where each voxel

correspond to one reconstructed diffraction pattern. By measuring multiple slices, 3D reconstruction of the patterns is possible. These reconstructed patterns are then treated the classical way where different components (phases) can be deconvoluted (same algorithm as in the previous example). However, now we have true 3D reconstruction instead of 2D map as in the previous example.

The reconstruction depicted in Figure 4 shows the different materials consisting the cell and in relation the water distribution across the membrane and within catalyst layer. The experiments discussed above are useful when the water movement within the cell need to be determined. However, such 3D reconstructions are currently time intensive (one 3D reconstruction takes about $1\,\mathrm{hr}$) and therefore this method is not yet practical for measuring dynamic water distribution.

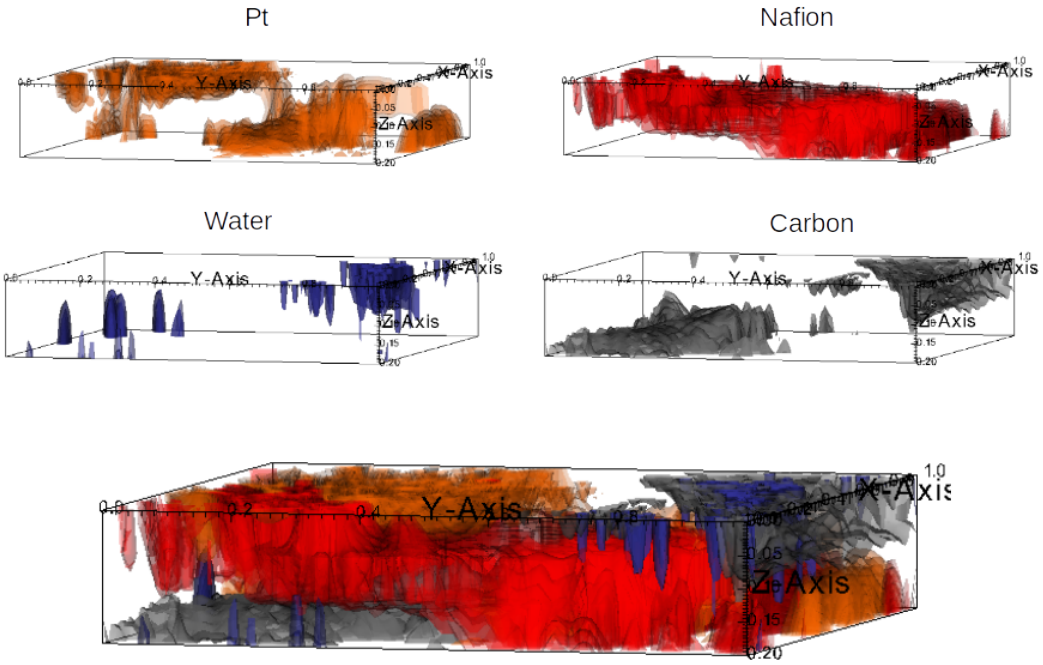

Figure 4: Tomographic reconstruction form XRD data of PEMFC constituent materials during the cell operation at $2\,\mathrm{A/cm^2}$

The XRD patterns reconstructed in previous example also provide information about the atomic arrangement within the materials. This can be used to conveniently determine the changes in the atomic structure of the catalyst layer induced by the functioning of the fuel cell. The catalyst layer is the most expensive part of the fuel cell and therefore chemical and structural stability is one of the major requirement. In Figure 5 are depicted structural parameters obtained from the Rietveld refinement of XRD tomography data. Scale factor is directly proportional to the amount of catalyst and can be used to determine the dissolution rate of the catalyst. Particle size and lattice parameter relate to the changes in morphology and chemical composition of the catalyst. All these information are needed to determine the operating conditions for the catalyst within the fuel cell, which can vary between materials and cell designs. This is of high importance for the proper device operation.

4 Conclusions

In the above, new approaches to study batteries and fuel cells in operando conditions are discussed. We show that using high energy X-rays combined with advanced analysis can provide useful information about the behaviour of the materials used in electrochemical devices and can help to fine-tune the device for maximum operation efficiency and safety.

Acknowledgments

The authors would like to thank staff of beamlines ID15a, ID19 and ID31 for their help during the experiments. Special thanks for Dr. Paul Shearing for for providing the materials for the experiment with exploding battery.

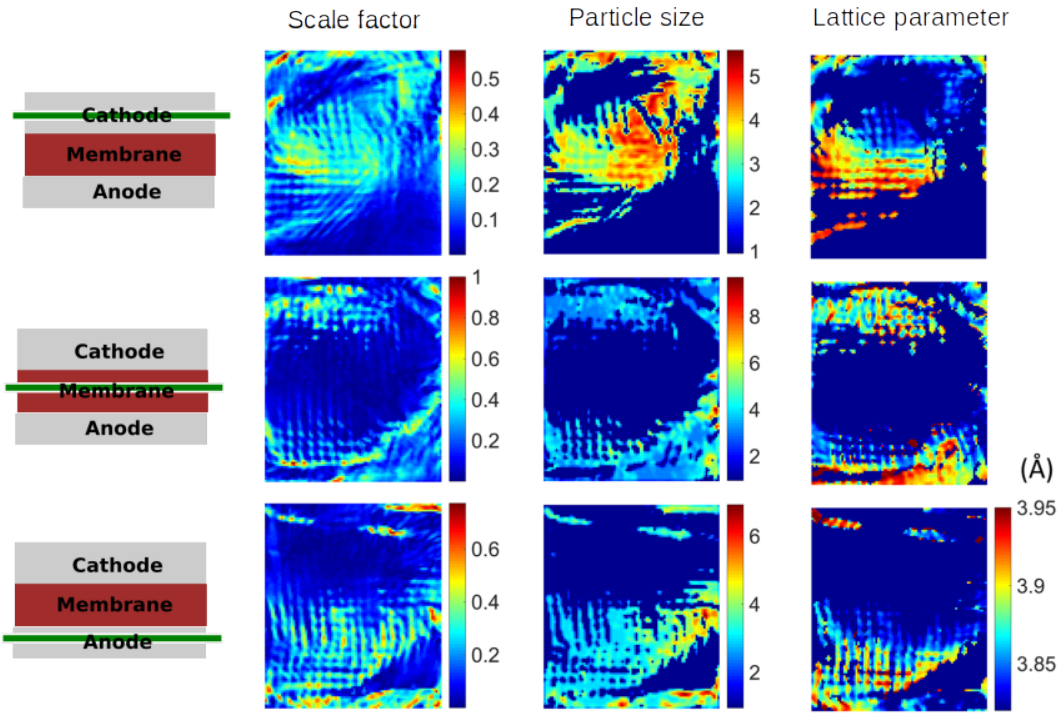

Figure 5: XRD tomographic reconstructions of PEMFC catalyst layer (Platinum). The scale factor of the Rietveld refinement is proportional to the amount of material. The particle size and the lattice parameter can be used to track the degradation of the catalyst during the operation.

References

[1] *ESRF*, http://www.esrf.eu, accessed on 2019-03-06.

[2] D.P. Finegan et al., *In-operando high-speed tomography of lithium-ion batteries during thermal runaway*, Nature Communications, 6(2015), 6924

[3] D.P. Finegan et al., *Characterising thermal runaway within lithium-ion cells by inducing and monitoring internal short circuits*, Energy Environ. Sci., 10(2017), 1377-1388

[4] K.M.O. Jensen et al., *X-Ray Diffraction Computed Tomography for Structural Analysis of Electrode Materials in Batteries*, J. Electrochem. Soc., 162(2015), A1310-A1314

[5] J. Sottmann et al., *Chemical Structures of Specific Sodium Ion Battery Components Determined by Operando Pair Distribution Function and X-ray Diffraction Computed Tomography.*, Angew. Chem. Int. Ed., 56(2017), 1138511389

Authors

Jakub Drnec He currently works as a beamline scientist at ID31and ID03 beamlines at ESRF. His background is in surface science, electrochemistry and 2D materials. His expertise is in advanced X-ray diffraction techniques and their application in the development of electrochemical conversion and storage devices.

Marco Di Michiel His main scientific activity is the development of new time resolved techniques for operando experiments in the field of Materials Chemistry. He pioneered dynamical micro-tomography as a time resolved

technique for in situ synchrotron experiments. Later he developed dynamical X-ray powder diffraction tomography and high energy stroboscopic X-ray diffraction.

Alexander Rack Scientist at the X-ray imaging beamline ID19 of the European Synchrotron Radiation Facility: X-ray optics characterisation, high-speed hard X-ray imaging, single-distance phase-retrieval, applications of microtomography, detector development.